Chemistry & Biology, Vol. 9, 1315–1321, December, 2002, ©2002 Elsevier Science Ltd. All rights reserved. PII S1074-5521(02)00282-X

Sequence-Dependent DNA Dynamics by Scanning Force Microscopy Time-Resolved Imaging

Anita Scipioni,[1,5] Giampaolo Zuccheri,[2,3,5] Claudio Anselmi,[1] Anna Bergia,[2,3] Bruno Samorì,[2,3,4] and Pasquale De Santis[1,4]
[1]Dipartimento di Chimica
Università "La Sapienza"
Roma
[2]Dipartimento di Biochimica G. Moruzzi
Università di Bologna
[3]INFM
Bologna
Italy

Summary

Scanning force microscopy was used to study in fluid the conformational fluctuations of two double-stranded DNA molecules resulting from differently cut *p*BR322 circular DNAs. A new approach was conceived to monitor the thermodynamic equilibrium of the chain dynamics on different scale lengths. This method made it possible to demonstrate that both the observed DNA molecules were allowed to equilibrate only on their local small-scale dynamics during the time of the experiment. This capability of monitoring the length scale and the time scale of the equilibration processes in the dynamics of a DNA chain is relevant to give an insight in the thermodynamics of the DNA binding with proteins and synthetic ligands. It was also shown that the small-scale equilibration of the DNA chain during surface-restricted dynamics is enough to allow a valid measurement of the local sequence-dependent curvature.

Introduction

DNA can be represented as a topologically conditioned elastic chain continuously fluctuating in solution under the thermal perturbations of the molecular environment. Its superstructural properties such as the sequence-dependent static and dynamic curvature are important for the management of the informational content, e.g., in protein-DNA association, transcription, replication, and recombination as well as in the writhing transitions of topologically constrained chains.

Different experimental methodologies were developed to study the DNA curvature and flexibility, like gel electrophoresis [1–6], circularization kinetics [7–10], electric dichroism [11], a statistical analysis of electron microscopy images [12], and scanning force microscopy (SFM) [13–15]. Significant progress was ensured by our recently reported statistical mechanics approach based on images of immobilized palindromic DNA dimers [16–18].

Additionally, SFM allows direct observation and study of the dynamics in solution of DNA single molecules deposited on an atomically flat surface. In the experiment here reported, we could study the large and the small-scale motions of a few kilobase pair (kbp) DNA molecules by analyzing their global shapes and their local sequence-dependent chain curvature and flexibility. It is expected that the time averaging of the molecular profiles assumed by a single molecule can replace the ensemble averaging of those of many immobilized molecules [17] and provide us with information on both the static and the dynamic sequence-dependent curvature. This is true, provided that our observation is long enough. In fact, the ergodic hypothesis in the Gibbs scheme allows us to replace the ensemble averages over all systems in an ensemble at a fixed time with time averages over a single system (when the course of time is long enough). Therefore, the SFM allows following the dynamics of a single DNA molecule in real time and opens an unexplored and very direct way for the study of the sequence-dependent mechanical properties of DNA.

The methods we have employed have been developed in the analysis of ensembles of static DNA molecules, for which we have shown that the sequence-dependent chain curvature and flexibility can be confidently measured and that the results are in good agreement with the theoretical predictions [17]. This new approach to the study of DNA superstructures could address the important issue of the rate of the large-scale structural changes of a DNA with respect to the local conformational changes, involving only relatively short DNA tracts, in particular when the environment severely restricts large-scale dynamics.

Both the intrinsic curvature and the flexibility along the sequence are found in satisfactory agreement with the theoretical predictions and with the results previously obtained by analyzing a large ensemble of static DNA molecules. Accordingly, the ergodicity of the local dynamics corresponding to fluctuations around the equilibrium (intrinsic) curvature was verified. On the contrary, the global shape of the DNA molecules shows a nonergodic behavior and a time evolution far from the equilibrium.

Results and Discussion

Quantitative SFM Study of the DNA Chain Dynamics and Equilibrium

Figure 1A shows three samples of SFM images out of a 4 hr time sequence observation of two linearized *p*BR322 DNA molecules. Each molecule is 1.5 μm long. Figures 1B and 1C show the superimposition of the traces from two time series of SFM images obtained by cutting two circular *p*BR322 DNA molecules (4.36 kbp) in two unknown positions. The images were recorded at time intervals of about 2 min and were superimposed by minimizing their central dispersion. It is evident from the figure that the global shapes of the two molecules are very different. As a measure of this, the average

[4]Correspondence: pasquale.desantis@uniroma1.it (P.D.S.), samori@alma.unibo.it (B.S.)
[5]These authors contributed equally to this work.

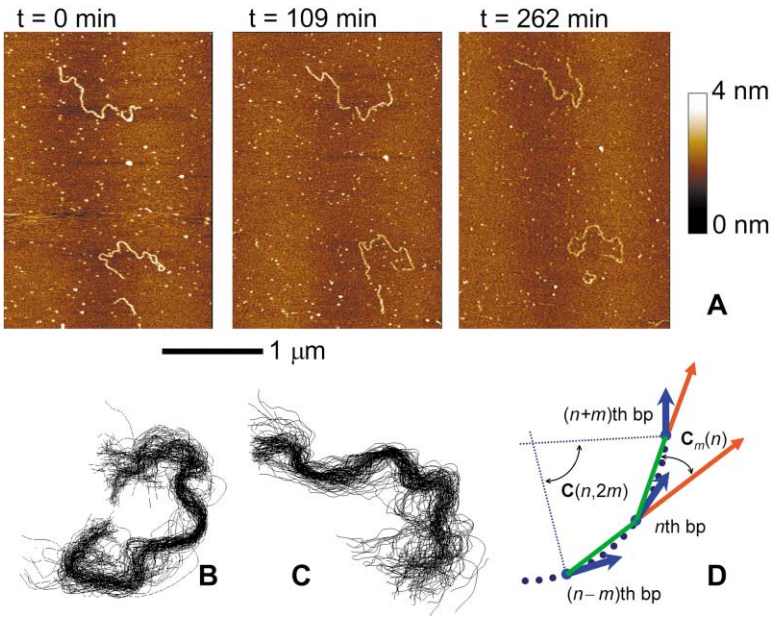

Figure 1. Examples of Data Acquisition and Digitalization

(A) Three samples of SFM images out of a 4 hr time-sequence observation of two linearized *p*BR322 DNA molecules. Each molecule is 1.5 μm long.

(B and C) Superimposition of 107 and 94 traces derived from SFM images of the two linearized *p*BR322 DNAs. The images were obtained at time intervals of about 2 min.

(D) Schematic representation of the segmental curvature, $C_m(n)$, at the sequence position n. It corresponds to the angle between the two virtual segments linking the $(n-m)$th nucleotide step with the nth, and the nth nucleotide step with the $(n+m)$th, respectively. $C_m(n)$ is half of the curvature $C(n,2m)$, which represents the angular deviation of the local helical axes pertinent to nucleotide steps separated by $2m$ bp.

squared end-to-end distances for the two molecules would correspond to apparent three-dimensional persistence lengths of 10 nm (Figure 1B) and 80 nm (Figure 1C) [14]. The discrepancy of these time averages from the accepted value for double-stranded DNA (50 nm) is so relevant that it cannot be explained by the different cut position of the original circular molecule. As evident from the shapes they assume over time (Figures 1B and 1C), the two molecules did not have enough freedom and time to equilibrate on the surface during the course of the experiment, so they could sample only a very limited portion of their accessible conformational space. Their global shape maintained a memory of the original state of adsorption on mica.

We have recently found a statistical mechanics relation to monitor the small-scale equilibration of DNA chains, evaluating their local curvature distribution [17, 18]. The proportionality between the small-scale curvature moduli and their standard deviations is theoretically predicted only in the case that the chains are at thermodynamic equilibrium (see Experimental Procedures). This correlation, found for an equilibrium statistical ensemble, should hold for the analysis of time-course data if the ergodic hypothesis is valid in the time of experiment. In addition, working on a single molecule guarantees that all the single-time curvature profiles refer to the same sequence with the same orientation.

As previously derived [17],

$$\langle |C_m(n)| \rangle = \left[\frac{2}{\pi} \left(\langle C_m(n) \rangle^2 + \frac{mRT}{2b(n)} \right) \right]^{1/2} \quad (1)$$

where $\langle |C_m(n)| \rangle$ is the time-average curvature modulus evaluated over m base pairs centered at the position n along the chain, and $\langle C_m(n) \rangle$ is the corresponding time-average curvature evaluated, taking into account the relative direction. This is equivalent to the static intrinsic curvature evaluated over a molecule ensemble. Counterintuitively, the time-averaged curvature modulus turns out to contain two types of contributions: one dependent on the intrinsic, static curvature, and one due to the chain flexibility. The curvature is considered as measured from the segmental-chain approximation of the DNA helix axis derived from SFM images (see Figure 1D). $b(n)$ is the apparent harmonic force constant of DNA at the nth position per nucleotide step proportional to the 3D local persistence length. The standard deviation of the average curvature modulus is:

$$SD(|C_m(n)|) = \left[\left(\frac{\pi - 2}{\pi} \right) \left(\langle C_m(n) \rangle^2 + \frac{mRT}{2b(n)} \right) \right]^{1/2} \quad (2)$$

The average curvature modulus and the relative standard deviation have the same dependence on both the intrinsic curvature and flexibility. They are proportional and their ratio is $(2/(\pi-2))^{1/2}$, contrary to the general feeling that associates only the flexibility to the curvature dispersions. Such a concept is correct exclusively when the curvature phases are taken into account [16, 17] (see Experimental Procedures).

The proportionality between the curvature moduli and their standard deviations was theoretically demonstrated under the assumption that the chains are at thermodynamic equilibrium. Therefore, this proportionality can be used as an internal gauge of the local equilibrium of DNA dynamics. We have already successfully tested this proportionality on a large statistical ensemble of stationary DNA molecule profiles [17].

Figure 2 shows the very similar profiles of the time-averaged curvature modulus and the corresponding standard deviation for the linearized *p*BR322 molecule whose time traces are shown in Figure 1B. The ratio of the curvature modulus along the chain and its standard deviation satisfactorily approximates the value predicted theoretically. This implies that on the scale of the evaluation of the curvature (about three helix turns in

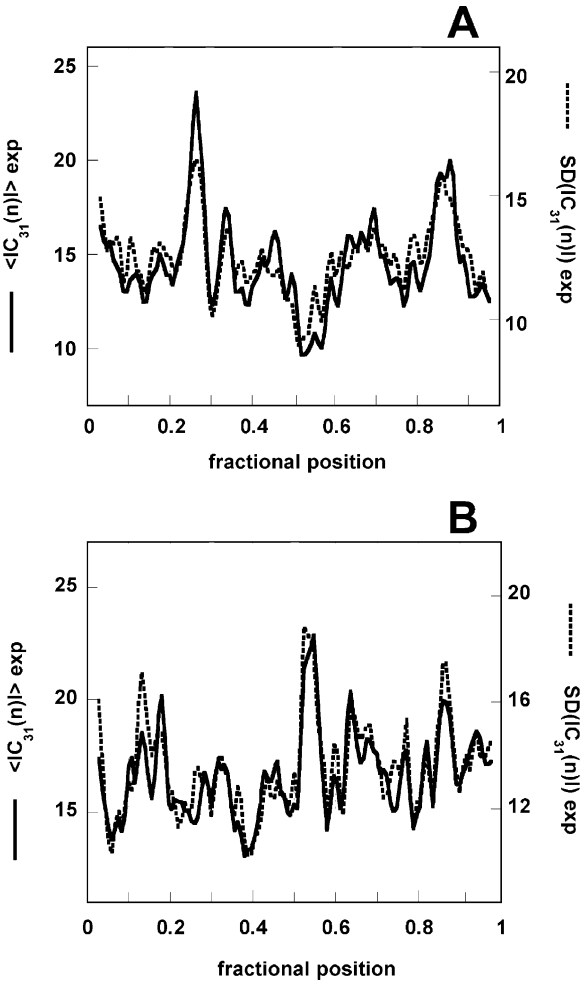

Figure 2. Comparison between the Local Time-Averaged Curvature Modulus and the Corresponding Standard Deviation

Comparison between the local time-averaged curvature modulus, $\langle|C_m(n)|\rangle$, and the corresponding standard deviation relative to the two linearized *p*BR322 molecules shown in Figure 1B (A) and in Figure 1C (B). All values are in degrees and refer to $m = 31$ bp (about three turns of the DNA helix).

the case shown), the chain segments have had enough time and mobility to sample the conformational space accessible to them and therefore can represent the corresponding equilibrium canonical ensemble. A similar result was obtained for the other molecule in Figure 1C.

Small-Scale and Large-Scale DNA Chain Dynamics

Figure 3 reports $\langle|C_m|\rangle$ versus the correspondent standard deviation; the values of the average ratio $\langle\langle|C_m|\rangle/SD(|C_m|)\rangle$, taken at regular intervals along the sequence of both the DNA molecules, monitor the ergodicity of the DNA dynamics. When the length, m, of the considered DNA segments increases, the ratios $\langle\langle|C_m|\rangle/SD(|C_m|)\rangle$ deviate from the theoretical value of $(2/(\pi-2))^{1/2}$, and their dispersion increases as well. This is quantified in Table 1. This finding clearly indicates that in the time of SFM experiments, equilibration is reached only for DNA tracts shorter than 60 bp. Therefore, the ergodicity is limited to ≈6 turns of DNA, and chain dynamics progressively become far from the equilibrium, at least within the time of the experiments. On the other hand, this evidence agrees with the increase of the relaxation time with the length of the chain. At the limit, it corresponds to the microscopic reversibility of the local conformational transformation following the Khinchin ergodic theorem [19].

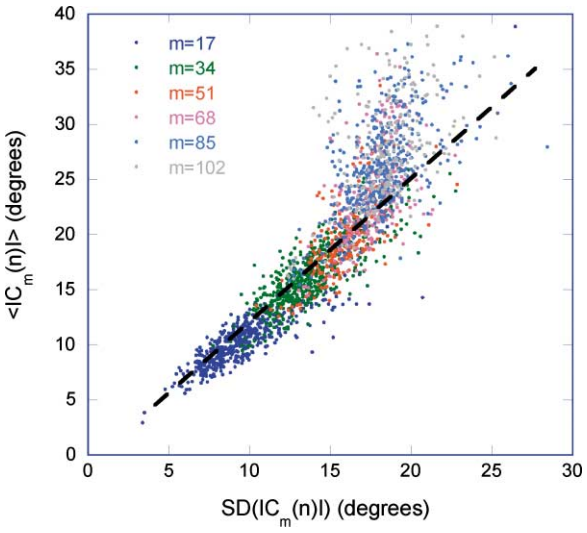

Figure 3. Time-Averaged Curvature Modulus versus the Corresponding Standard Deviation for Different DNA Segment Lengths

Time-averaged curvature modulus, $\langle|C_m|\rangle$, and the relative standard deviation, $\langle SD(|C_m|)\rangle$, for different DNA segment lengths, m, averaged for the two linearized *p*BR322 molecules shown in Figure 1.

An evaluation of the standard deviation of the chain curvature on the same size scale allows the calculation of an average 3D persistence length of 51 nm (according to Equation 10 in Experimental Procedures). This is in good agreement with the most common value found with different techniques and experiments (transient electric birefringence, TEB; transient electric dichroism, TED; electron microscopy, and circularization) and further confirms the local ergodicity of the DNA chains in the conditions of the experiment. A very similar value of the 3D persistence length we found in previous analysis of SFM images of large statistical ensembles of different DNA molecules. The higher values reported in literature [20], as obtained by TEB experiments in low-salt solution, suggest that the effective ionic strength nearby the mica surface is higher than in the solution used [21] and reduces the low-salt persistence length to the limit value of about 50 nm at higher salt. On the other hand, it should be noted that different experimen-

Table 1. Ratios of the Average Curvature Modulus and the Relative Standard Deviation for Different DNA Tract Lengths

m (bp)	$\left\langle \frac{\langle\|C_m\|\rangle}{SD(\|C_m\|)} \right\rangle$
34	1.22 ± 0.12
51	1.32 ± 0.15
68	1.38 ± 0.17
85	1.45 ± 0.19
102	1.48 ± 0.21

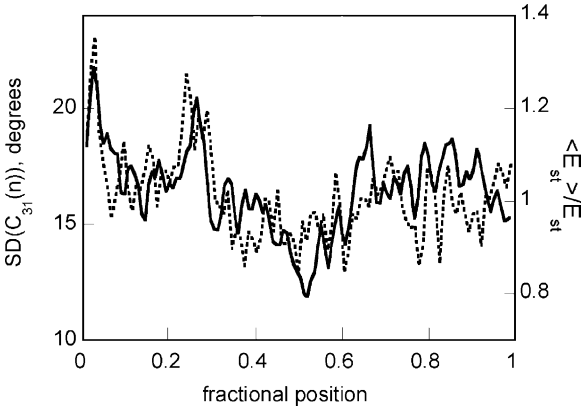

Figure 4. Comparison between Experimental Curvature Standard Deviation and Sequence-Dependent Differential Flexibility

Comparison between the experimental curvature standard deviation, SD(C_{31}(n)), measured over three DNA turns and the sequence-dependent differential flexibility relative to the molecule in Figure 1B. The sequence-dependent differential flexibility is represented by the reciprocal values of the normalized theoretical stacking energy of the dinucleotide steps [24].

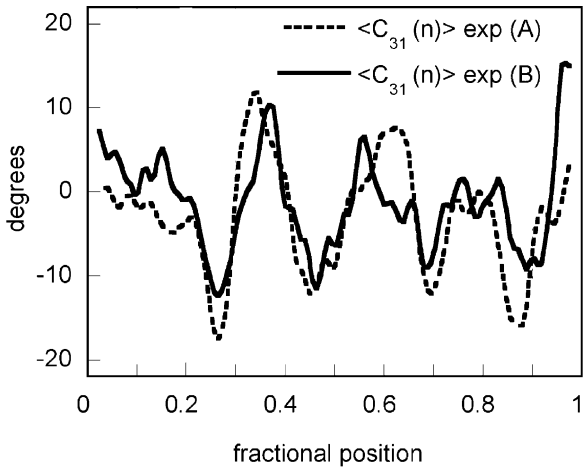

Figure 5. Time-Averaged Curvature of the Two *p*BR322 Molecules

The profiles of the time-averaged curvature relative to the two molecules shown in Figures 1B and 1C are superimposed after cyclically permutating one with respect to the other to find the maximum of the correlation function.

tal techniques and theoretical models as well as temperature and DNA curvature provide different values of persistence length, as recently reviewed [22].

Therefore, the local chain dynamics seems to represent the corresponding equilibrium statistical ensemble, in spite of the apparent invalidity of the ergodic hypothesis for the large-scale chain dynamics as monitored by the nonstandard values of the end-to-end distances. This is due to the limited time intervals of the SFM observations under the adsorption conditions. Accordingly, Figure 4 shows the satisfactory comparison between the standard deviation of the curvature along the sequence and the corresponding differential flexibility as represented by the reciprocal normalized stacking energy of the dinucleotide steps [23, 24]. As first suggested by Hagerman [20], the main contribution to the differential stability of the DNA structure with different sequences is the base-pair stacking energy.

In spite of the large differences in their global shapes, Figure 5 shows that the two molecules have similar time-averaged local curvature profiles (taking also into account the relative signs of the curvatures) after a cyclic permutation corresponding to the maximum of the correlation function. A careful study of the average time curvature of the two molecules under analysis has shown that the measured small-scale curvatures are in satisfactory agreement with the sequence-dependent local curvatures that can be theoretically predicted for *p*BR322. Figure 6 illustrates the comparison between the experimental curvature profiles of the two molecules as reported in Figure 5 and the theoretical profile. The theoretical curvature was calculated using the dinucleotide step orientational parameters previously proposed [23, 24] and cyclically permuted to maximize the corresponding correlation. As a result, the sequence of the two molecules can be defined, and the cutting sites of the circular *p*BR322 DNA can be identified through the comparison of the curvature patterns.

It turns out that the global shape of a DNA molecule has little influence on the measured local chain curvature, which instead depends only on the base sequence, provided that the curvature evaluation is made on a thermodynamically equilibrated data set. The intrinsic curvature information that can be gathered even from a limited time series of data can be enough to characterize a DNA sequence and permit a sequence alignment.

Significance

This paper provides insight into the problem of the time evolution of DNA curvature in terms of the se-

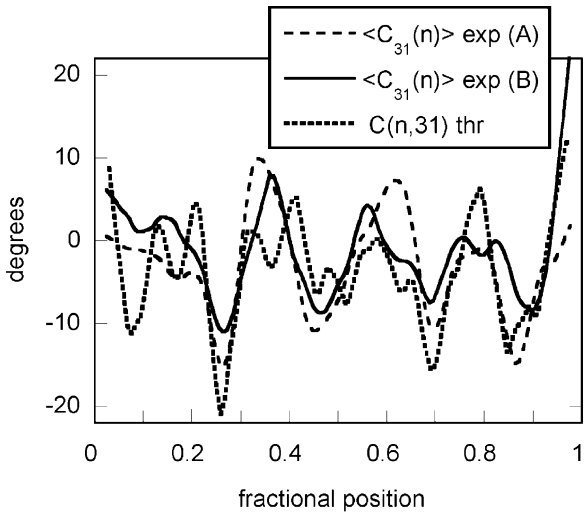

Figure 6. Comparison between the Experimental and the Theoretical Curvature

Comparison between the experimental and the theoretical curvature profiles relative to the molecules in Figures 1B and 1C. The theoretical curvature was calculated using the dinucleotide step orientational parameters previously proposed [23, 24] and cyclically permuted to optimize the corresponding correlation.

quence on the basis of time-resolved SFM images. Both the time-average intrinsic curvature and flexibility along the sequence are in satisfactory agreement with the theoretical predictions, based on a sequence-dependent model of the DNA curvature and flexibility we previously advanced [23]. The results support the ergodicity of the local dynamics, corresponding to fluctuations around the equilibrium (intrinsic) curvature. On the contrary, they indicate that the global shape of the DNA molecules has a nonergodic behavior and a time evolution far from the equilibrium. This raises the question of whether the structural and/or chemical transformations involving DNA can be considered among thermodynamic equilibrium states. In this sense, protein binding as well as local interactions can be considered as equilibrium thermodynamic processes, because any memory of the starting conformation is quickly lost at local scale. On the other hand, could the large-scale DNA transformations be represented by equilibrium processes in the time scale involved in biological processes? This is not true for *p*BR322 dynamics on the mica surface in a time interval of several hours, since they conserve memory of their starting shapes. In the case of longer genomic DNAs, the problem of the apparent conservation of the DNA architecture is even more dramatic, suggesting that the dynamic pathway of replication mechanisms guarantees not only the conservation of the genome but also a significant part of the DNA architecture. From a methodological point of view, SFM single-molecule method opens the possibility of directly studying the local physical properties of DNA molecules even in the presence of proteins or other ligands.

Experimental Procedures

SFM Imaging of DNA in Solution

Fluid SFM imaging was performed on a NanoScope III SFM (Digital Instruments, Santa Barbara, CA) equipped with a multimode head. A commercial tapping-mode fluid cell (Digital Instruments) was employed with electron-beam-deposited SFM probes built according to the method reported by Keller [25] on silicon nitride triangular cantilevers with a nominal force constant of 0.38 N/m. *p*BR322 plasmid molecules were deposited on a disc of freshly cleaved ruby mica (Mica New York Corp., NY) for approximately 1 min from a 1 μg/ml DNA solution that contained 4 mM HEPES, 1 mM $MgCl_2$ (pH 6.8–7.4). After the deposition time, MilliQ deionized water (Millipore) was injected into the assembled fluid cell. SFM imaging was performed in tapping mode at an oscillation frequency slightly lower than the maximum of a low-frequency oscillation peak (lower than 10 kHz) [26]. The linear scanning speed was 5–10 μm/s for a sampling density of 15–30 nm^2/pixel.

Measure of Local DNA Curvature and Flexibility from the SFM Images

Raw SFM images have been processed only for background removal (flattening) using the microscope manufacturer's image-processing software. DNA molecule profiles have been measured from the SFM images using ALEX, a software package written for probe microscopy image processing [14], by semiautomatically tracking the molecule contours on the SFM images.

In digitizing the molecule contours, we have left out molecules with suspiciously short contour length (probably fragments) and a few that had suspiciously long contour lengths.

The distribution of the pixel file, which interpolates the DNA chain, was normalized via Fourier transform operations. These convert the nonuniform pixel sequence of the DNA images into a uniform coordinate distribution along the contour length. After this transformation, the number of points, which interpolate the DNA traces, remains practically invariant and corresponds to the average value of pixels per molecule. The curvature angles were evaluated from the vectorial product of overlapping directional chain segments. The resulting curvature functions were averaged, and the corresponding standard deviation was calculated for different segment lengths.

Theoretical Evaluation of the Local DNA Curvature and Flexibility

Sequence-Dependent Curvature and Flexibility from a Statistical Mechanics Analysis of SFM Images

According to the classical formulation by Landau and Lifshitz [27], the curvature of a space line is defined as the derivative $C = dt/d\ell$ of the tangent versor, t, along the line, ℓ. In the case of DNA, the line corresponds to the helical axis, and the curvature is a vectorial function of the sequence. It represents the angular deviation between the local helical axes of the nth and $(n + 1)$th helix turns centered on the nth and $(n + 1)$th dinucleotide step, respectively.

A simple model was first advanced based on conformational energy minimization of the ten independent dinucleotide steps, which provided an evaluation of the differential deviation angles from the standard B-DNA [23, 24]. We introduced a simple evaluation of the differential curvature along the DNA sequence as

$$\mathbf{C}_o(n) = \frac{1}{\nu_n} \sum_{n\text{th turn}} \mathbf{d}_s \exp\left(\frac{2\pi i s}{\nu_n}\right), \tag{3}$$

where $\mathbf{C}_o(n)$ is the intrinsic curvature per base pair at the nth position of the sequence, $\mathbf{d}_s = \rho_s - i\tau_s$ is the complex representation of the roll and tilt angles at the sth position, and ν_n is the corresponding local helical periodicity. The summation is extended iteratively to each turn of double helix and is assigned to the middle base pair.

Such a formulation of the intrinsic sequence-dependent curvature function in the complex plane represents in modulus and phase the local deviation of the DNA helical axes from the straight direction.

To take into account the dynamic curvature fluctuations, we modified [23, 24] the previous formulation by introducing a time dependence of the local base pair orientational deviations as

$$\mathbf{C}(n,t) = \frac{1}{\nu_n} \sum_{n\text{th turn}} [\mathbf{d}_s + \delta_s(t)] \exp\left(\frac{2\pi i s}{\nu_n}\right) =$$

$$\mathbf{C}_0(n) + \frac{1}{\nu_n} \sum_{n\text{th turn}} \delta_s(t) \exp\left(\frac{2\pi i s}{\nu_n}\right) = \mathbf{C}_0(n) + \chi(n,t). \tag{4}$$

$\delta_s(t)$ is generally a time- and sequence-dependent quantity increasing with the flexibility, whereas $\chi(n,t)$ represents the contribution of the time-dependent curvature. Therefore, the instant curvature differs from the intrinsic static curvature for the second term. This term, however, always vanishes by time averaging. The second-order distribution of time fluctuations $\langle|\chi(n)|^2\rangle_t$ does not vanish and therefore can be observed as time average.

Adopting first-order elasticity and according to Landau and Lifshitz [27], we define the bending distortion energy of a m bp DNA tract as

$$\Delta E_b = \frac{1}{2} \sum_1^m b(n) |\chi(n,t)|^2. \tag{5}$$

$b(n)$ represents the apparent harmonic force constant per nucleotide step at position n of the sequence.

Therefore, adopting the first-order elasticity for DNA axis deformations and setting $B = b(n)/2RT$, we define the elastic partition function of a DNA ensemble as

$$Q(n) = \int \exp(-B|\chi(n)|^2) d\chi(n), \tag{6}$$

and the curvature dispersion at the nth position becomes

$$\langle|\chi(n)|^2\rangle = \frac{1}{Q(n)}\int|\chi(n)|^2\exp(-B|\chi(n)|^2)d\chi(n) = \frac{1}{B} \quad (7)$$

according to the Hagerman result in solution [20]. It should be noted that in 3D, $\chi(n)$ is a vectorial quantity and the integration is made in the complex plane.

However, when DNA is forced on a 2D surface as in SFM, the curvature becomes a real quantity and the lower dimensionality of chain halves the curvature dispersion. Furthermore, due to SFM resolution limits, a DNA molecule is generally represented as a segmental chain. Therefore, we introduce a new parameter to characterize the curvature, $C_m(n)$, corresponding to the angle between the m bp virtual segments at a sequence position, n, as well as the corresponding deviation, $\chi_m(n)$. Such a segmental curvature $C_m(n)$ is half of the curvature $C(n,2m)$, which represents the angular deviation of the local helical axis pertinent to nucleotide steps separated by $2m$ bp as illustrated in Figure 1. The latter can be theoretically calculated, while the first one is what we experimentally measure. Therefore, we introduce the curvature as a function of both the position n and the length of virtual segments, m.

The relative dispersion is

$$\langle\chi^2(n,2m)\rangle = \frac{1}{Q(n,2m)}\int_{-\infty}^{\infty}\chi^2(n,2m) \times \exp\left(-\frac{B}{2m}\chi^2(n,2m)\right)d\chi(n,2m) = \frac{m}{B} \quad (8)$$

where

$$Q(n,2m) = \int_{-\infty}^{\infty}\exp\left(-\frac{B}{2m}\chi^2(n,2m)\right)d\chi(n,2m). \quad (9)$$

Therefore, the experimentally measured $\chi_m^2(n)$ is $\chi^2(n,2m)/4$, since it depends on the curvature fluctuations of $2m$ bp, and its square root is

$$SD(C_m(n)) = \left(\frac{mRT}{2b(n)}\right)^{1/2}. \quad (10)$$

The standard deviation of the curvature only depends on the differential flexibility along DNA sequence.

On the contrary, the average curvature modulus contains both the static and the dynamic curvature contributions, i.e., it is related to both the intrinsic curvature and the curvature fluctuations which involve $2m$ bp. It can be calculated as a suitable approximation for curvatures of interest, and the following compact formulation is obtained for $\langle|C_m(n)|\rangle$:

$$\langle|C_m(n)|\rangle = \frac{\langle|C(n,2m)|\rangle}{2} = \left[\frac{2}{\pi}\left(\langle C_m(n)\rangle^2 + \frac{mRT}{2b(n)}\right)\right]^{1/2}. \quad (11)$$

This result clearly points out that the average curvature modulus depends on two terms: one is the intrinsic curvature and the other one represents the sequence-dependent flexibility of the chain. Adopting the same approximation, we obtain the standard deviation of curvature modulus:

$$SD(|C_m(n)|) = \left(\langle C_m^2(n)\rangle - \langle|C_m(n)|\rangle^2\right)^{1/2} = \left[\left(\frac{\pi-2}{\pi}\right)\left(\langle C_m(n)\rangle^2 + \frac{mRT}{2b(n)}\right)\right]^{1/2}. \quad (12)$$

Unexpectedly, both the average curvature modulus and the relative standard deviation have the same dependence on the intrinsic curvature and flexibility. They are proportional and their ratio is $(2/(\pi-2))^{1/2}$. Conversely, the experimental outcome of such proportionality can work as an internal gauge of the local equilibrium of DNA dynamics. Therefore, in the conditions of validity of the ergodic theorem for time fluctuations involving m bp, we can extend the formulation obtained for the ensemble averages to the time averages of a single DNA molecule dynamics. Conversely, the experimental finding of the proportionality of the average curvature modulus and the relative standard deviation, as in Equations 11 and 12, proves the existence of a thermodynamic equilibrium at the local scale.

Acknowledgments

The authors would like to thank Carlos Bustamante for useful discussion. This work was supported by Programmi Biotecnologie Legge 95/95 (MURST) 5%, MURST Progetti di Ricerca di Interesse Nazionale 1999–2001 and 2001–2003, "Progetto 60% Ateneo" of University "La Sapienza," Progetto Pluriennale Università di Bologna e.f. 2001, and Fondazione Pasteur Cenci-Bolognetti.

Received: June 10, 2002
Revised: September 30, 2002
Accepted: October 15, 2002

References

1. Marini, J.C., Levene, S.D., Crothers, D.M., and Englund, P.T. (1982). Bent helical structure in kinetoplast DNA. Proc. Natl. Acad. Sci. USA *79*, 7664–7668.
2. Wu, H.M., and Crothers, D.M. (1984). The locus of sequence-directed and protein-induced DNA bending. Nature *308*, 509–513.
3. Koo, H.S., Wu, H.M., and Crothers, D.M. (1986). DNA bending at adenine-thymine tracts. Nature *320*, 501–506.
4. Hagerman, P.J. (1985). Sequence dependence of the curvature of DNA: a test of the phasing hypothesis. Biochemistry *24*, 7033–7036.
5. Hagerman, P.J. (1986). Sequence-directed curvature of DNA. Nature *321*, 449–450.
6. Koo, H.S., and Crothers, D.M. (1988). Calibration of DNA curvature and a unified description of sequence-directed bending. Proc. Natl. Acad. Sci. USA *85*, 1763–1767.
7. Shore, D., Langowski, J., and Baldwin, R.L. (1981). DNA flexibility studied by covalent closure of short fragments into circles. Proc. Natl. Acad. Sci. USA *78*, 4833–4837.
8. Shore, D., and Baldwin, R.L. (1983). Energetics of DNA twisting. I. Relation between twist and cyclization probability. J. Mol. Biol. *170*, 957–981.
9. Kahn, J.D., and Crothers, D.M. (1992). Protein induced bending and DNA cyclization. Proc. Natl. Acad. Sci. USA *89*, 6343–6347.
10. Roychoudhury, M., Sitlani, A., Lapham, J., and Crothers, D.M. (2000). Global structure and mechanical properties of a 10-bp nucleosome positioning motif. Proc. Natl. Acad. Sci. USA *97*, 13608–13613.
11. Hagerman, P.J. (1996). Sometimes a great motion: the application of transient electric birefringence to the study of macromolecular structure. Curr. Opin. Struct. Biol. *6*, 643–646.
12. Muzard, G., Theveny, B., and Revet, B. (1990). Electron microscopy mapping of *p*BR322 DNA curvature. Comparison with theoretical models. EMBO J. *9*, 1289–1298.
13. Bednar, J., Furrer, P., Katritch, V., Stasiak, A.Z., Dubochet, J., and Stasiak, A. (1995). Determination of DNA persistence length by cryo-electron microscopy. Separation of the static and dynamic contributions to the apparent persistence length of DNA. J. Mol. Biol. *254*, 579–594.
14. Rivetti, C., Guthold, M., and Bustamante, C. (1996). Scanning force microscopy of DNA deposited onto mica: equilibration versus kinetic trapping studied by statistical polymer chain analysis. J. Mol. Biol. *264*, 919–932.
15. Zuccheri, G., Dame, R.Th., Aquila, M., Muzzalupo, I., and Samorì, B. (1998). Conformational fluctuations of supercoiled DNA molecules observed on real time with a scanning force microscope. Appl. Phys. A: Mater. Sci. Process *66*, S585–S589.
16. Zuccheri, G., Scipioni, A., Cavaliere, V., Gargiulo, G., De Santis, P., and Samorì, B. (2001). Mapping the intrinsic curvature and flexibility along the DNA chain. Proc. Natl. Acad. Sci. USA *98*, 3074–3079.

17. Scipioni, A., Anselmi, C., Zuccheri, G., Samorì, B., and De Santis, P. (2002). Sequence-dependent DNA curvature and flexibility from scanning force microscopy images. Biophys. J. *83*, 2408–2418.
18. Sampaolese, B., Bergia, A., Scipioni, A., Zuccheri, G., Savino, M., Samorì, B., and De Santis, P. (2002). Recognition of the DNA sequence by an inorganic crystal surface. Proc. Natl. Acad. Sci. USA 99, 13566–13570.
19. Khinchin, A.I. (1949). Mathematical Foundation of Statistical Mechanics. (New York: Dover).
20. Hagerman, P.J. (1988). Flexibility of DNA. Annu. Rev. Biophys. Biophys. Chem. *17*, 265–286.
21. Samorì, B., Muzzalupo, I., and Zuccheri, G. (1996). Deposition of supercoiled DNA on mica for scanning force microscopy imaging. Scanning Microsc. *10*, 953–962.
22. Lu, Y., Weers, B., and Stellwagen, N.C. (2002). DNA persistence length revisited. Biopolymers *61*, 261–275.
23. De Santis, P., Palleschi, A., Savino, M., and Scipioni, A. (1990). Validity of the nearest-neighbor approximation in the evaluation of the electrophoretic manifestations of DNA curvature. Biochemistry *29*, 9269–9273.
24. Anselmi, C., De Santis, P., Paparcone, R., Savino, M., and Scipioni, A. (2002). From the sequence to the superstructural properties of DNAs. Biophys. Chem. *95*, 23–47.
25. Keller, D.J., and Chou, C.-C. (1992). Imaging steep, high structures by scanning force microscopy with electron beam deposited tips. Prog. Surf. Sci. *268*, 333–339.
26. Schabert, F.A., and Rabe, J.P. (1996). Vertical dimension of hydrated biological samples in tapping mode scanning force microscopy. Biophys. J. *70*, 1514–1520.
27. Landau, L.D., and Lifshitz, E.M. (1970). Theory of Elasticity (Oxford, NY: Pergamon Press).